Inorg. Chem. **2006**, 45, 6844–6850

Inorganic Chemistry
Article

A Novel Zn^{II}-Sensitive Fluorescent Chemosensor Assembled within Aminopropyl-Functionalized Mesoporous SBA-15

Ling Gao,[†] Ying Wang,*[,†] Jianqiang Wang,[†] Li Huang, Liying Shi,[†] Xiaoxing Fan,[‡] Zhigang Zou,*[,‡] Tao Yu,[‡] Mei Zhu,[‡] and Zhaosheng Li[‡]

School of Chemistry and Chemical Engineering, Nanjing University, Nanjing 210093, China, and Eco-materials and Renewable Energy Research Center, Nanjing University, Nanjing 210093, China

Received September 26, 2005

A novel Zn^{2+}-sensitive fluorescent chemosensor SC/SBA-15 has been obtained by the self-assembly of 4-chloroaniline-*N*-salicylidene (SC), a Schiff base ligand, within the channel of silylation-modified SBA-15 without destroying its hexagonally ordered mesoporous structure. The remarkable 200-fold fluorescence enhancement with a large Stokes shift of 180 nm in luminescence emission upon the addition of Zn^{2+} is attributed to the formation of a coordinate complex of a large rigid conjugate system and Zn^{2+} ions.

Introduction

The design of a highly selective and sensitive fluorescent chemosensor for the detection of Zn ions has attracted considerable attention because Zn is one of the essential and vital components in environmental and biological systems.[1−7] In general, a rationally designed chemosensor consists of a reception unit and a signaling unit. Once the target metal ion binds to the π-electron system of the receptor, some significant changes to the photophysical properties of the chromo- or fluorophore (signal unit) such as hypso- or bathochromic modulations of absorption and emission enhancement or quenching occur, thus realizing the “recognition” for the target metal ion. On the basis of this “binding site−signaling unit” approach, several fluorescent sensors are synthesized for selective recognition and quantitive analysis of Zn^{2+} at the nanomolar to micromolar level.[8−11] To gain a strong fluorescent signal, quinoline and fluorescein chromophores are commonly chosen as the signaling unit. For the acceptor, piperidine tripod and macrocyclic polyamine were used as the binding unit to form a stable complex of metal ions.[12−18] However, some of these promising chemosensors suffer from different drawbacks such as high basal fluorescence and slow complex formation rate because of the inherent properties of the macrocyclic polyamine. Accordingly, some efforts to anchor the fluorophore and receptor units on inorganic support have been made and led to some novel optical hybrid sensors.[19,20] In the present study, an attempt at assembly of a small fluorescent chromophore that possesses a coordinative conjugation π-electron system

---

[*] To whom correspondence should be addressed. E-mail: wangy@nju.edu.cn (Y.W.).

[†] School of Chemistry and Chemical Engineering.

[‡] Eco-materials and Renewable Energy Research Center.

(1) Paker, M. M.; Humaller, F. L.; Mahler, D. J. *Clin. Chem.* **1967**, *13*, 40.
(2) Vallee, B. L.; Falchuk, K. H. *Physiol. Rev.* **1993**, *73*, 79.
(3) Berg, J. M.; Shi, Y. *Science* **1996**, *271*, 1081.
(4) Choi, D. W.; Koh, J. Y. *Annu. Rev. Neurosci*. **1998**, *21*, 347.
(5) Weiss, J. H.; Sensi, S. L.; Koh, J. Y. *Trends Pharmacol. Sci*. **2000**, *21*, 395.
(6) Canzoniero, L. M. T.; Turetsky, D. M.; Choi, D. W. *J. Neurosci*. **1999**, *19*, RC31.
(7) Gee, K. R.; Zhou, Z.-L.; Qian, W.-J.; Kennedy, R. *J. Am. Chem. Soc*. **2002**, *124*, 776.
(8) Hendrickson, K. M.; Geue, J. P.; Wyness, O.; Lincoln, S. F.; Ward, A. D. *J. Am. Chem. Soc.* **2003**, *125*, 3889.
(9) Shults, M. D.; Pearce, D. A.; Imperiali, B. *J. Am. Chem. Soc.* **2003**, *125*, 10591.
(10) Chang, C. J.; Nolan, E. M.; Jaworski, J.; Okamoto, K.-I.; Hayashi, Y.; Morgan, S.; Lippard, S. L. *Inorg. Chem.* **2004**, *43*, 6774.
(11) Kawabata, E.; Kikuchi, K.; Urano, Y.; Kojima, H.; Akira, O.; Nagano, T. *J. Am. Chem. Soc.* **2005**, *127*, 818.
(12) Savage, D. D.; Montano, C. Y.; Kasarskis, E. J. *Brain Res.* **1989**, *496*, 257.
(13) Zalewski, P. D.; Forbes, I. J.; Betts, W. H. *J. Biochem.* **1993**, *296*, 403.
(14) Walkup, G. K.; Burdette, S. C.; Lippard, S. L.; Tsien, R. Y. *J. Am. Chem. Soc.* **2000**, *122*, 5644.
(15) Burdette, S. C.; Walkup, G. K.; Spingler, B.; Tsien, R. Y.; Lippard, S. J. *J. Am. Chem. Soc.* **2001**, *123*, 7831.
(16) Hirano, T.; Kikuchi, K.; Urano, Y.; Higuchi, T.; Nagano, T. *Angew. Chem., Int. Ed.* **2000**, *39* (6), 1052.
(17) Komatsu, K.; Kikuchi, K.; Kojima, H.; Urano, Y.; Nagano, T. *J. Am. Chem. Soc.* **2005**, *127*, 10197.
(18) Hirano, T.; Kikuchi, K.; Urano, Y.; Higuchi, T.; Nagano, T. *J. Am. Chem. Soc.* **2000**, *122*, 12399.
(19) Brasola, E.; Mancin, F.; Rampazzo, E.; Tecilla, P.; Tonellato, U. *Chem. Commun.* **2003**, 3026−3027.

10.1021/ic0516562 CCC: $33.50

thus can act as both an acceptor and a signaling precursor on the functionalized inner surface of the porous inorganic support was actualized by strong guest−host interaction. Anchoring of this small organic chromophore on the designated binding sites of a porous inorganic support is expected to provide a facilitative coordination environment.

Considering that the more rigid conjugate structure of a compound tends to generate stronger fluorescence,[21] we designed a chemosensor containing a small Schiff base fluorescent chromophore moiety and functionalized mesoporous SBA-15 that possesses a rigid inner surface. A relatively small ligand molecule, owing to its lower steric hindrance, tends to fast complexing with the targeted ions. Also, the rigid surface of solid support, after being linked to a conjugate fluorescent chromophore moiety, will increase the total rigidity of the sensor system. Mesoporous SBA-15, a hexagonally ordered mesoporous silica, first prepared by Zhao et al. through cohydrolysis and ploy condensation of a nonionic surfactant ethylene oxide/propylene oxide triblock copolymer (P123) and tetraethyl orthosilicate (TEOS) under acidic conditions,[22] is chosen as the sensor scaffold because it can supply a rigid inner surface by silylation on its silicon wall. Though SBA-15 itself is nonfluorescent, it is suitable as a sensor scaffold because it can supply a high surface area covered with a layer of hydroxyl groups that can act as binding sites for covalent grafting of silanes on a silicon wall. The use of a versatile silylation reagent not only rigidifies the inner surface of the mesoporous silica by cross linking O into the Si−O framework[23] but also introduces the active functional groups such as amino or halogen groups that are useful for further functionalization.

The aminopropyl-group-functionalized siliceous material has been used for further covalent or noncovalent anchoring of some chromogenic fluorescent molecules.[24,25] The strong interaction between the guest fluorescent molecules and the functionalized inner surface of SBA-15 increases the rigidity of the hybrid complex, which favors the generation of a strong fluorescent signal. Yet, the ordered one-dimensional straight channel and larger pore size (up to 30 nm) of SBA-15 facilitate the lowering of the diffusion resistance and the enhancement of accessibility, which is very significant in the application. Particularly, the reason that SBA-15 can supersede other mesoporous materials is that its ordered structure can be maintained after occlusion of guest molecules, which results from the thicker wall that aids in the maintainance of the structural integrity. Moreover, using a siliceous host as a solid binding unit has inherent advantages such as optical transparency in the visible region and favorable biocompatibility, which enables such silica-based materials to be promising sensor substrates.[26−30]

To introduce a terminal amine group $-NH_2$ inside the channel of SBA-15, we chose (aminopropyl)triethoxysilane [APTES, $NH_2(CH_2)_3Si(C_2H_5O)_3$] as the silylation reagent to rigidify the mesoporous framework. To the best of our knowledge, there is no report on the assembly of a Zn^{2+}-sensitive chemosensor based on mesoporous material SBA-15. This prompts us to report herein our fluorescent chemosensor for Zn^{2+} synthesized by self-assembly of a relatively small chromophore within the channels of trialkoxysilane-derivatized mesoporous SBA-15. Transmission electron microscopy (TEM), UV−vis spectrophotometry, and fluorescence spectrometry were used to characterize the hybrid mesoporous material.

Experimental Section

Reagents and Chemicals. Pluronic P123, an ethylene oxide (EO)/propylene oxide (PO) triblock copolymer with composition $EO_{20}PO_{70}EO_{20}$ and with an average molecular weight of 5800, was purchased from Aldrich. Tetraethyl orthosilicate (TEOS), the silica source, (aminopropyl)triethoxysilane (APTES), parachloroaniline, salicylaldehyde, and aniline were procured from Nanjing Chemical Reagent Company (China). $Zn(CH_3COO)_2$ and the other metal salts were provided by Shanghai Fourth Chemical Reagent Company (China). All of the reagents and solvents were of analytical reagant grade and were used as received, except aniline, which was distilled in a vacuum just before use.

Synthesis and Aminopropyl Functionalization of SBA-15. Mesoporous silica SBA-15 was prepared according to the literature by using a triblock copolymer as the template.[22] In a typical synthesis, 2.0 g of triblock P123 was dissolved in 60 mL of 2 M aqueous HCl and 15 mL of distilled water under stirring, and then 4.4 g of TEOS was added dropwise to the solution at room temperature. The mixture was stirred for 24 h at 313 K, and then the temperature was raised to 373 K and kept at 373 K for another 24 h in a Teflon-lined autoclave. Finally the resulting precipitate was filtered, washed carefully with distilled water, air-dried, and calcined at 773 K in air for 5 h to remove the template and to obtain the final product SBA-15.

The aminopropyl functionalization of SBA-15 was carried out by using APTES [$NH_2(CH_2)_3Si(C_2H_5O)_3$] as the silylation reagent. About 0.5 g of powder SBA-15 was mixed with a 25-mL chloroform solution of APTES (0.2 M) and stirred for 12 h at room temperature, and then the precipitate was filtered and washed with chloroform. The solid product was air-dried and denoted as APTES/SBA-15.

Preparation of 4-Chloroaniline-*N*-salicylidene and Aniline-*N*-salicylidene. Parachloroaniline (1.28 g, 0.01 mol) was dissolved in 15 mL of absolute alcohol at room temperature at first, and then 1.5 g of salicylaldehyde (0.01 mol) was added dropwise into the solution. The mixture was stirred at room temperature for 2 h, and

---

(20) El Haskouri, J.; Ortiz de Zárate, D.; Guillem, C.; LaTorre, J.; Caldés, M.; Beltrán, A.; Beltrán, D.; Descalzo, A. B.; Rodríguez-López, G.; Martínez-Máñez, R.; Marcos, M. D.; Amorós, P. *Chem. Commun.* **2002**, 330−331.

(21) Nijegorodov. N. I.; Downey, W. S. *J. Phys. Chem.* **1994**, *98*, 5639.

(22) Zhao, D. Y.; Feng, J. L.; Huo, Q. S.; Melosh, N.; Fredrickson, G. H.; Chmelka, B. F.; Stucky, G. D. *Science* **1998**, *279*, 548.

(23) Xu, W.; Guo, H.; Akins, D. L. *J. Phys. Chem. B* **2001**, *105*, 1543.

(24) Subramanian, A.; Kennel, S. J.; Oden, P. I. *Enzyme Microb. Technol.* **1999**, *24*, 26.

(25) Descalzo, A. B.; Jiménez, D.; Haskouri, J. E.; Beltrán, D.; Amorós, P.; Marcos, M. D.; Máñez, R.; Soto, J. *Chem. Commun.* **2002**, 562.

(26) Panchard, M. S.; Huber, R.; Renault, M.; Maas, H.; Pansu, R.; Calzaferri, G. *Angew. Chem., Int. Ed.* **2001**, *40*, 2839.

(27) Lin, V. S. Y.; Lai, C. Y.; Huang, J.; Song, S. A.; Xu, S. *J. Am. Chem. Soc.* **2001**, *123*, 11510.

(28) Beck, C.; Hartl, W.; Hempelmann, R. *Angew. Chem., Int. Ed.* **1999**, *38* (9), 1297.

(29) Descalzo, A. B.; Rurack, K.; Weisshoff, H.; Manez, R.; Dolores, M.; Amoros, P.; Hoffmann, K.; Sato, J. *J. Am. Chem. Soc.* **2005**, *127*, 184.

(30) Xu, W.; Akins, D. L. *J. Phys. Chem. B* **2002**, *106*, 1991.

the obtained luminescent orange crystalloid was filtered and purified by recrystallization in 20 mL of absolute alcohol twice. Finally, the obtained product 4-chloroaniline-*N*-salicylidene, denoted as SC, was air-dried, and the total yield achieved was 78%. ^{1}H NMR ($CDCl_3$, 300 MHz): δ_H 8.62 (1 H), 7.42 (4 H), 7.26 (2 H), 7.03 (2 H), 6.97 (1 H). Chemical shifts are expressed in ppm. Electrospray ionization mass spectrometry (ESI-MS) confirmed the $[M]^+$ peak (with data *m*/*z* 232.2) of SC. IR data: ν_{max} (KBr pellets)/cm^{-1} 3427 (br, OH), 3054 (m, CH, arom), 2980 (m, CH), 2907 (m, CH), 1610 (s, $-CH{=}N-$), 1485 (m, CH, arom), 1456 (m, CH, arom), 759 (m, CH, arom), 518 (m, C−Cl, arom). The same synthetic procedure was used to prepare aniline-*N*-salicylidene (denoted as SA), and the only exception was the reactant. Aniline was employed instead of parachloroaniline.

Preparation of SC/SBA-15 and SA/SBA-15 Composites. For a typical preparation, 25 mg of SC was dissolved in 38 mL of ethanol at first, and then 0.5 g of APTES-modified SBA-15 was mixed in the solution for 24 h at room temperature. The suspension was centrifuged and the transparent aqueous solution decanted, while the residue was carefully washed with anhydrous ethanol to remove SC molecules from the external surface. After the suspension was air-dried, a yellowish solid product was obtained and designated as SC/SBA-15. Another composite, SA/SBA-15, was prepared in a similar preparation process.

Instruments and Spectroscopic Measurements. The ^{1}H NMR experiments were performed on a set of Bruker DPX-300 spectrometers at 298 K, and $CDCl_3$ was used as the solvent. All chemical shifts are reported in the standard δ notation of ppm; positive chemical shifts are denoted to higher frequency from the given reference. ESI-MS analyses were carried out at the Finnigan mat LCQ liquid chromatography (LC)/MS coupling technique. The IR spectra were obtained on a Bruker Vector 22, and the sample was mixed with KBr at a ratio of 3:97 (w/w) and then pressed as a thin disk for testing. The TEM image was acquired on a JEOL JEM-100S electron microscope. Samples were levigated, suspended in ethanol, and dispersed on a Cu net by ultrasound for TEM investigations.

Steady-state fluorescence spectra were acquired on a Varian-Cary Eclips spectrofluorometer at room temperature. All spectrophotometric titrations were performed with a suspension of the sample dispersed in a ethanol/water (9:1, v/v) solution (pH 7.0), and then the sample was brought into a quartz cell for measurement. The fluorescence quantum yield was obtained by comparison of the integrated area of the emission spectrum and the absorbance of the samples with the reference under the same excited wavelength. The concentration of the reference L-tryptophan ($\Phi = 0.14$) in an aqueous solution was adjusted to match the absorbance of the test sample. The quantum efficiency of a metal-bound sample was measured by using a solid suspension solution of 0.1 g/L SC/SBA-15 and 5×10^{-5} M Zn^{2+}. Emission for Zn-SC/SBA-15 was integrated from 380 to 550 nm with excitation at 250 nm, whereas for Zn-free SC/SBA-15, the emission area was integrated from 280 to 450 nm. The quantum yields were calculated with eq 1.[31]

$$\Phi_{\text{sample}} = \Phi_{\text{reference}} \frac{\int \text{emission}_{\text{sample}}}{\int \text{emission}_{\text{reference}}} \frac{A_{\text{reference}}}{A_{\text{sample}}} \tag{1}$$

For measurements of the fluorescence lifetime, the experiments were performed on one set of time-resolved fluorescence spectrometers (TRFSs), SLM 48000DSCF/AB2 (SLM INC America). The pulse train was synchronously pumped by the frequency doubling of a HeCd laser.

Scheme 1. Synthesis of SC and SA

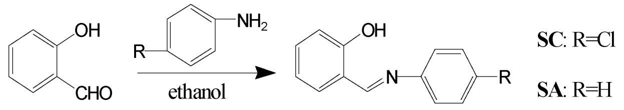

UV−vis diffuse-reflectance absorption spectra of the opaque powders were recorded under ambient conditions from 200 to 600 nm on a Shimadzu UV-2401PC spectrophotometer adapted with a praying mantis attachment and using $BaSO_4$ as the reference. Reflectance spectra were converted to Kubelka Munk values *F*(*R*) that correlate with on-loaded APTE/SBA-15.

Combustion chemical analyses (C, H, and N) of the silicates containing organic material were carried out in a CHNO− Rapid (Germany) elemental analyzer.

Results and Discussion

Synthesis and Characterization of the Hybrid Material. We prepared the organic ligand SC first. The ^{1}H NMR results confirmed the existence of five kinds of H in the molecular structure of the product, and the IR spectrum revealed the $-C{=}N-$ stretching vibration band at 1610 cm^{-1} that is characteristic of this Schiff base. In addition, the strong molecular ion peak with a *m*/*z* value of 232 was detected in a ESI-MS spectrum, indicating the formation of the desired Schiff base ligand.

To explore the impact of the Cl group in the reactant parachloroaniline on the anchoring of SC guest molecules on APTES/SBA-15, we also prepared another Schiff base ligand, SA, under the same reaction conditions (see Scheme 1), except aniline was used as the reactant instead of parachloroaniline. The Cl-connected aromatic ring may change the electronic cloud density of the reactant molecule through its inherent electron-withdrawing or donation effect from its lone-pair electron. Figure 1 depicts the corresponding UV−vis diffuse reflectance spectra of SC and SA crystals, in which a broad adsorption band centered at about 408 nm, resulting from the $\pi \rightarrow \pi^*$ electronic transition of the Schiff base molecule,[3232] is observed on the spectrum of both SC and SA. A new adsorption band, as a clear shoulder, emerges at around 520 nm in the spectrum of SC (curve B in Figure 1) but is absent in the spectrum of SA (curve A in Figure 1). This band at 520 nm can probably be attributed to the $n \rightarrow \pi^*$ electronic transition occurring in the SC molecule because both the π-electron conjugate system and the lone-pair electron (nonbonded) of the Cl groups that usually act as auxochromes coexist in this molecule. The higher energy level of nonbonded lone-pair electron of the Cl group would reduce the band gap of the molecular orbital and thus result in the new adsorption band at 520 nm.

To facilitate the incorporation of a SC or SA chromophore moiety within the channel of mesoporous SBA-15, it is necessary to modify the interface of the host first to promote the proper guest−host interaction.[32,33] Thus, we modified the

---

(31) Parker, C. A.; Rees, W. T. *Analyst* **1960**, *85*, 587.

(32) Zhang, H.; Zhang, P.; Ye, K.; Sun, Y.; Jiang, S.; Wang, J.; Wang, Pang, W. *J. Lumin.* **2006**, *117*, 68.

(33) Zhao, X. S.; Lu, G. Q. *J. Phys. Chem. B* **1998**, *102*, 1556.

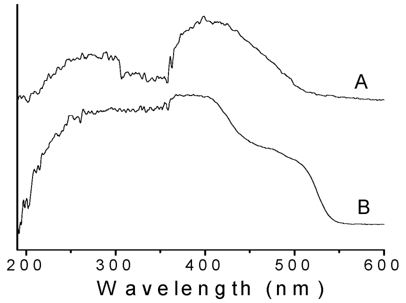

Figure 1. UV−vis diffuse-reflectance spectra of (A) SA and (B) SC samples.

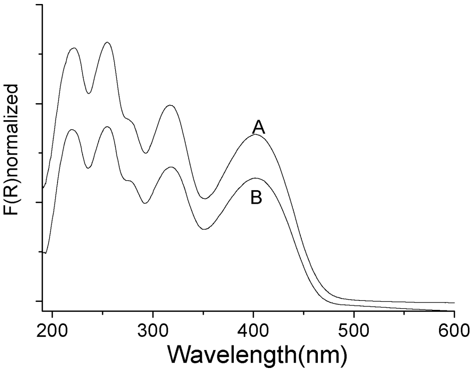

Figure 2. UV−vis spectra of (A) SA/SBA-15 and (B) SC/SBA-15.

surface of SBA-15 by using a silylation reagent, APTES, which can covalently link organosilane species (aminopropyl groups) through Si−O−Si bonds to the internal surface and rigidify the mesoporous framework.[33] Also, such a rigid surface will serve as a suitable scaffold for the assembly of a chemosensor. Another advantage of using a postgrafting method is the high density of amine groups obtained in the porous host. For those samples directly synthesized by the one-pot method, the density of the amine groups is usually between 0.5 and 2.3 mmol/g,[34,35] whereas CHN analysis revealed that a high amino group density, up to 3.54 mmol/g, is obtained on our sample APTES/SBA-15 prepared through the postgrafting method. These amino groups should act as binding sites for further anchoring of guest molecules in mesoporous silica and assembly of an effective chemosensor.

Encapsulation of a SC or SA ligand within the channel of APTES-functionalized SBA-15 was performed in an alcohol solution of the ligand at room temperature. On the basis of the results of EA, about 2.5×10^{-5} mol/g of SC is loaded on the support, which is much less than that of the amine groups assembled in SBA-15. Figure 2 compares the UV−vis diffuse-reflectance spectra of SA/SBA-15 and SC/SBA-15 powder samples. As expected, a series of characteristic bands of the Schiff base at 222, 254, 316, and 402 nm emerge in the spectra of both SA/SBA-15 and SC/SBA-15 with a higher resolution, implying the successful incorporation of a SC or SA ligand into SBA-15. These bands can be attributed to the typical electronic transition of an aromatic ring and −C=N− conjugate system in a Schiff base molecule.[31,35,36] However, it is noteworthy that the adsorption band at 520 nm, which is assigned to the n → π^* electronic transition, disappears from the spectrum of SC/SBA-15 after the SC ligand is encapsulated into the APTES-functionalized SBA-15. This is presumably related to the electronic effect between the Cl groups of the SC molecule and the aminopropyl groups of APTES/SBA-15. After anchoring into APTES/SBA-15, the strong guest−host interaction results in partial charge transfer (lone-pair electron) from the Cl group on an aromatic ring to the proton of the pendent aminopropyl groups of APTES/SBA-15, which thus hinders the n → π^* electronic transition.

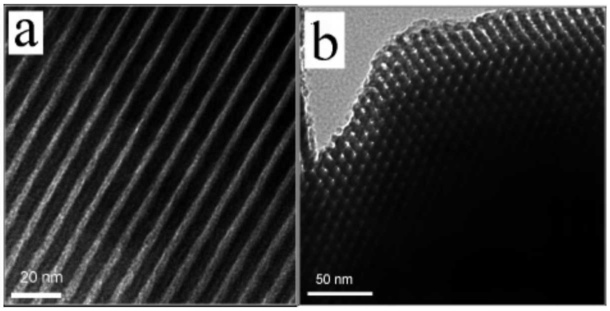

Figure 3. TEM image of SC/SBA-15 (a) in the direction perpendicular to the pore axis and (b) in the direction of the pore axis.

The structure of our hybrid composite SC/SBA-15 is examined by means of high-resolution TEM (HRTEM), and Figure 3 confirms the high mesoscopic order of the SC/SBA-15 composite. This material exhibits a hexagonal array of ordered channels and the typical honeycomb resembling that of SBA-15. The pore size of the calcined SBA-15 sample is estimated to be ca. 6 nm according to the N adsorption−desorption isotherm, and the introduction of a putative monolayer of the silylation reagent APTES on SBA-15 narrows the pore size to ca. 3.5 nm. This narrowness in the pore size contributed to the occupation of organosilanes on those APTES-functionalized SBA-15 samples, which possess a high density of amine functional groups.[35] Nonetheless, this pore diameter is still large enough to allow the SC molecules with approximate dimensions of ca. 1.2 nm × 0.5 nm (calculated by the *Gaussian98* suite of programs) to be incorporated into the modified SBA-15.

To further pursue the interaction between the ligand guest and APTES/SBA-15 host, the photophysical properties of SC-anchored APTES/SBA-15 along with the recognition of the resulting complexes for the Zn^{2+} ion were studied. For these tests, very dilute solutions of SC ($c = 5 \times 10^{-5}$ M) in ethanol/water (9:1, v/v) at pH 7.0 and a SC/SBA-15 or SA/SBA-15 complex ($c = 0.1$ g/L, corresponding to a concentration of the SC chromophore of 2.5×10^{-6} M) were used to measure the fluorescence emission spectra, respectively. Also, the fluorescence titration with Zn^{2+} ions and the quantum yield were measured under the same conditions.

Figure 4 compares the fluorescence spectra of a SC ligand before and after being anchored into APTES-modified SBA-15. The emission band (excitation 230 nm) of SC appears

---

(34) Maria, A. S.; Zhao, X. S. *J. Phys. Chem. B* **2003**, *107*, 12650.

(35) Wang, X. Q.; Lin, S. K.; Chan, C. C.; Cheng, S. *J. Phys. Chem. B* **2005**, *109*, 1763.

(36) Sutra, P.; Brunel, D. *Chem. Commun.* **1996**, 2485.

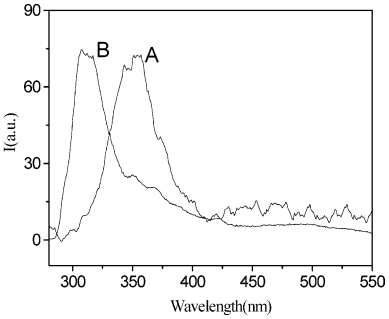

Figure 4. Fluorescence spectra of (A) SC, 5×10^{-5} M (excited at 230 nm), and (B) SC/SBA-15, 0.1 g/L (excited at 248 nm), dissolved or suspended in an ethanol/water solution (9:1, v/v).

at 350 nm (curve A in Figure 4), whereas a typical emission band (excitation 248 nm) emerges at 315 nm in the spectrum of SC/SBA-15 (curve B in Figure 4), which characterizes a significant blue shift after the SC molecules are anchored in the channel of APTES/SBA-15. Such a blue-shift phenomenon was also observed in the emission spectra of TSPP-encapsulated APTES/MCM-41[23] and interpreted in terms of the interaction between the sulfonato groups of an organic chromophore and the aminopropyl groups of APTES/MCM-41 in this host−guest system, which is also connected to steric effects associated with the pore structure of the modified MCM-41. Zhang et al. studied the photophysical properties of Schiff base molecules encapsulated in the channel of MCM-41[37] and found an obvious blue shift of anchored Schiff base molecules in comparison with pure ligands. They interpreted this phenomenon by the molecular orbital confinement theory that all energy levels of guest molecules increase in the channel of the host as a result of the confinement. Both MCM-41 and SBA-15 belong to the mesoporous silica possessing the ordered channels, so that their geometric confinements on the organic molecules should be similar. Consequently, the reason that the blue shift in our experiments may be the same as that reported by Zhang et al. is that in our hybrid complex the increase in the energy level of the SC molecule probably results in the blue shift on the spectrum of SC/SBA-15.

To compare the recognition ability of the SC/SBA-15 and SA/SBA-15 complexes for Zn^{2+}, their fluorescence spectra were recorded at room temperature. Once a trace of Zn^{2+}, available as acetate, was added into the suspension [ethanol/water (9:1, v/v)] of SC/SBA-15 (0.1 g/L), a new strong fluorescence emission, centered at 430 nm (curve A in Figure 5) with about a 200-fold fluorescence intensity and a larger Stokes shift of 180 nm, immediately appeared in the spectrum of SC/SBA-15 apart from the original emission at 315 nm. However, the luminescence response of SA/SBA-15 to the Zn^{2+} cation dramatically differs from that of SC/SBA-15. As is evident from Figure 5 (curve B), no emission at 430 nm is observed in the spectrum of SA/SBA-15 after the Zn^{2+} cation was added into its suspension. This unusual fluorescence enhancement at 430 nm mirrors the key role of Cl on the phenyl groups of the Schiff base.

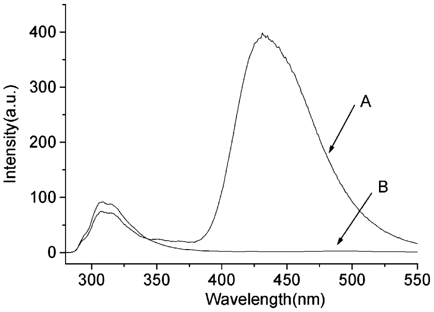

Figure 5. Fluorescence spectra of (A) SC/SBA-15 and (B) SA/SBA-15, 0.1 g/L with Zn^{2+} (5×10^{-5} M; excited at 248 nm), suspended in an ethanol/water solution (9:1, v/v).

Scheme 2. Schematic Representation of SC Self-assembly within the Channel of APTES-Modified Mesoporous Silica SBA-15

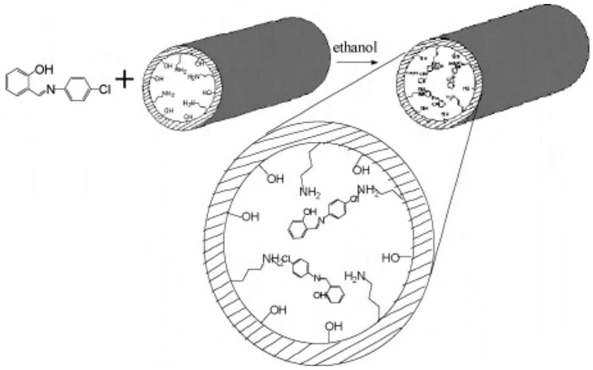

As is well-known, the aromatic nucleophilic substitutions are usually not feasible unless the reactants are activated by some strong electron-withdrawing groups ortho and para to the leaving group or the reaction is catalyzed by a very strong base.[38] However, in the molecule of Schiff base SC, a π-electron conjugate system containing a phenol and a −C═N− electron fluid bridge is ortho to the Cl on the phenyl, which makes the nucleophilic substitution of Cl difficult. Therefore, direct attachment of aminopropyl groups to the aromatic ring of SC seems very difficult. In comparison with the fluorine of fluorobenzene that can act as a π-electron donor and possess a strong proton affinity,[39] however, the Cl group in the SC molecule is an efficient π-electron donor because of its large ionic radius and shares a high electron density of the conjugate system, which enables the Cl group to possess a strong proton affinity. Also, correspondingly, the H of aminopropyl groups acts as an π-electron acceptor or a “H bridge” to link the SC molecule to the APTES-modified SBA-15, and thus a large rigid π system forms. Owing to this strong interaction between the Cl group of the SC fluorophore and the amino group of triethoxysilane-modified SBA-15, SC molecules can self-assemble on the pore wall of the host, as is demonstrated in the amplified view of Scheme 2, which enhances the whole rigidity of the ensemble containing SC and the interface of APTES/SBA-15.

Judging the structural difference between SC and SA molecules, it is reasonable to speculate that the replacement

---

(37) Zhang, L.; Xiong, Y.; Cheng, P.; Tang, G.; Zheng, D. *Chem. Phys. Lett.* **2002**, *358*, 278.

(38) March, J. *Advanced Organic Chemistry*, 4th ed.; John Wiley & Sons: New York, 1992.

(39) Carroll, T. X.; Thomas, D. T.; Henrik, B.; Børve, K. J.; Sæthre, L. J. *J. Org. Chem.* **2006**, *71* (5), 1961.

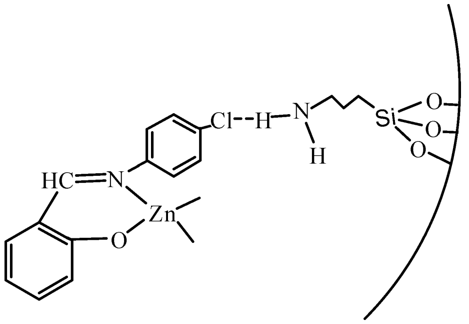

Chart 1. Schematic Representation of a Coordination Complex of Zn^{2+} and SC/SBA-15

of Cl on the phenyl of SC by H will make the molecule lose its π-electron-donating ability or proton affinity. Thus, encapsulation of SA in APTES/SBA-15 is only a physical loading process, and subsequently no rigid π-electron system is established. The nonemission at 430 nm in the fluorescence spectrum of SA/SBA-15 after the addition of excess Zn^{2+} confirms this envisagement.

The fluorescence enhancement at 430 nm provides the relevant structural information on the complexation of Zn^{2+} cations with SC/SBA-15. We also titrated Zn^{2+} in the solution containing only APTES-modified SBA-15 or SC, but no emission at 430 nm in the spectrum was observed (spectra not shown). These facts hint at the structure of the strong emissive complex, in which Zn^{2+} may coordinate to a whole large rigid π system consisting of a conjugated SC and APTES/SBA-15 ensemble, as shown in Chart 1. The amino groups, acting as the acceptor of the H bond to link with the SC Schiff base, are involved in the formation of the strong fluorescent complex Zn^{2+}-SC/SBA-15.

Without complexation with Zn^{2+}, free SC only produces a fluorescence emission at 350 nm, which is probably due to the radiated transition of $\pi-\pi^*$ ($S_0 \rightarrow S_1$). Upon complexation of the Zn^{2+} ion, photoinduced electron transfer (PET) is hindered by use of the lone pair of N of the $-C{=}N-$ groups in a large rigid π-electron system. This system works in a way similar to that found in some aminofluoresceins[16,20] and is explained as the depression of the highest occupied molecular orbital level due to the electron-donating group complex formation with a cation involving the lone-pair electron of N in the $-C{=}N-$ groups. In addition, the coordination of Zn^{2+} to the whole large π-electron system containing a Schiff base and the aminopropyl-functionalized inner surface of SBA-15 may increase the rigidity of the fluorescent SC molecule. Yet, this metal binding may alter the relaxation processes from the excited state, e.g., radiative decay and interconversion. Thus, our current results suggest that both the conformational restriction of the rigid conjugate system and the binding-induced electron transfer from the N atom in the $-C{=}N-$ groups and the O atom in the phenol to a metal ion are attributed to the fluorescence enhancement of SC/SBA-15 for the Zn^{2+} cation.

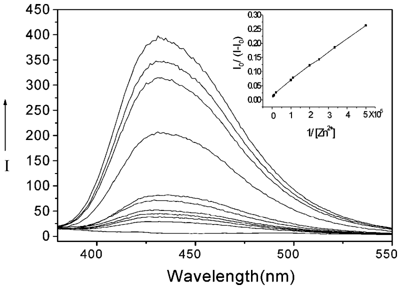

Figure 6. Fluorescence spectral changes of SC/SBA-15 (c = 0.1 g/L) with different concentrations of Zn^{2+} in an ethanol/water (9:1, v/v; pH 8.0) solution. The inset shows the plot of $I_0/(I - I_0)$ vs $[Zn^{2+}]^{-1}$. Excitation wavelength: 248 nm.

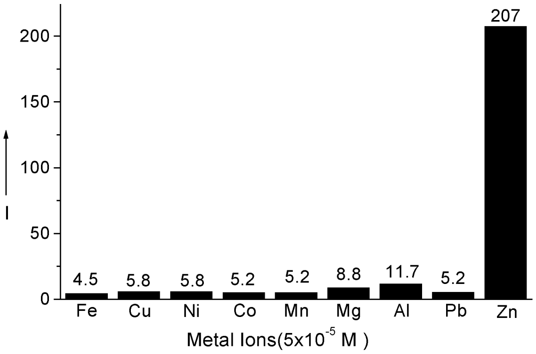

Figure 7. Luminescence intensity of SC/SBA-15 with metal ions in an ethanol/water solution (9:1, v/v; pH 8.0). Excitation wavelength: 248 nm.

Figure 6 illustrates the emission response of the chemosensor SC/SBA-15 via the Zn^{2+} concentration. The emission intensity at 420 nm increases monotonically with a slight "blue shift" throughout the addition of the target cation Zn^{2+} into the solution, while the shape of the emission band remains constant in these spectra. The inset in Figure 6 shows the plot of $I_0/(I - I_0)$ vs $[Zn^{2+}]^{-1}$, where I_0 and I refer to the emission at 430 nm for SC/SBA-15 in the absence and presence of Zn^{2+}, respectively. On the basis of these results, a good linearity between the fluorescence emission intensity and the concentration of Zn^{2+} is constructed (linearly dependent coefficient: $R^2 = 0.987$) in the detection range of 1−50 μM/L. The detection limit in the ethanol/water (9:1, v/v) system by use of 0.1 g/L SC/SBA-15 is calculated to be about 0.2 ng/mL. In the absence of Zn^{2+}, the quantum yield of SC/SBA-15 is 0.12, whereas it increases significantly to 0.47 in the presence of 5×10^{-5} M Zn^{2+} with the fluorescence lifetime of 3.68 ns. This means that Zn cation binding leads to an increase of the fluorescence quantum yield. The quantum yield of SC/SBA-15 for Zn^{2+} is slightly higher than that of $ZnAF_1$ and $ZnAF_2$, at 0.23 and 0.36, respectively.

The fluorescence of SC/SBA-15 is stable in the pH range of 7−8 and then monotonically increases to the maximum at pH 13. This dependence of fluorescence on the pH is consistent with the character of a PET mechanism-based benzylic amine-type chemosensor.[17]

The selectivity of the chemosensor toward other cations was examined. Ag^+, Ca^{2+}, Co^{2+}, Cu^{2+}, Fe^{3+}, Mn^{2+}, K^+, Na^+, Mg^{2+}, Al^{3+}, Ni^{2+}, Pb^{2+}, Sr^{2+}, Ba^{2+}, Cr^{3+}, and Zn^{2+} ions were used, at a concentration of 5×10^{-5} M, to evaluate the metal ion binding, and all of the titration studies were conducted by fluorescence enhancement, with Zn^{2+} among these metal ions at $\lambda_{max(em)} = 430$ nm.[40,41] As is evident from Figure 7, a small enhancement in fluorescence is detected upon the addition of Co^{2+}, Cu^{2+}, Fe^{3+}, Mg^{2+}, Al^{3+}, Ni^{2+}, Pb^{2+}, and Mn^{2+} ions of 5.0×10^{-5} M, whereas there is almost no response to some other metal ions of Ag^{+}, K^{+}, Na^{+}, Ca^{2+}, Sr^{2+}, Ba^{2+}, Cd^{2+}, and Cr^{3+}. On the basis of these results, it is very likely that our fluorescent chemosensor SC/SBA-15 is a highly sensitive and selective sensor for Zn^{2+} in an ethanol/water solution. Especially, it is noteworthy that, unlike the other Zn^{2+} sensors,[18,42] fluorescent sensors SC/SBA-15 demonstrated excellent competence for distinguishing Cd^{2+} and Zn^{2+}. Such exclusivity of SC/SBA-15 for Zn^{2+} is rather elusive by the outer electronic structures of those ions. Further studies designed to utilize other porous material as a substrate-binding unit are in progress.

In summary, we have reported a novel turn-on type Zn^{2+}-selective fluorescent chemosensor that is obtained by self-assembly of a small organic ligand SC within the channel of silylation-modified SBA-15. A remarkable enhancement in the luminescence emission of SC/SBA-15 upon the addition of Zn^{2+} is attributed to the formation of a coordinate complex of a large rigid conjugate system to Zn^{2+} ions. Further efforts will focus on the development of a new robust fluorescent chemosensor by using diversified porous materials as a promising sensor scaffold.

Acknowledgment. Financial support from NSFC (Grants 20273031 and 20373024) and the Analysis Center of Nanjing University is gratefully acknowledged. The authors thank Dr. D. Wu of the Department of Material Science of Nanjing University for the HRTEM experiments.

IC0516562

---

(40) Nakahara, Y. S.; Kida, T.; Nakatsuji, Y.; Akashi, M. *Chem. Commun.* **2004**, 224.

(41) Kim, J. S.; Noh, K. H.; Lee, S. H.; Kim, S. K.; Yoon, J. *J. Org. Chem.* **2003**, *68*, 597.

(42) Lim, N. C.; Schuster, J. V.; Porto, M. C.; Tanudra, M. A.; Yao, L.; Freake, H. C.; Bruckner, C. *Inorg. Chem.* **2005**, *44* (6), 2018.